ENGINEERING TRANSACTIONS • *Engng. Trans.* • **40**, 4, 469–481, 1992
Polish Academy of Sciences • Institute of Fundamental Technological Research

LARGE PLANE DYNAMIC POSTCRITICAL DEFORMATIONS OF ELASTIC BEAM

Z. WESOŁOWSKI and J. WIDŁASZEWSKI (WARSZAWA)

Large elastic deformations of a prismatic beam with inextensible axis are analysed. The beam at rest is an elastic arch formed by buckling from an initially straight beam and fixing its ends. The beam is modelled as a system of rigid elements connected by means of elastic hinges. The resulting motion equations are integrated numerically. The initial-boundary problem is solved with the use of Lagrange multipliers at each time step. Static characteristics are obtained with the use of the dynamic relaxation method.

1. Description of the problem

When an elastic beam is subject to large flexure and then fixed at its ends, an elastic arch is formed as shown in Fig.1. One of the features of such a nonlinear system is the existence of two configurations of stable equilibrium. Flat springs based on this idea have been known to have numerous applications in technology, especially in various fixing and positioning devices. They are usually made of thin metal sheet with a high elastic limit which ensures a reversible behaviour within a broad range of deflections and curvatures. One of the applications consists in capability of the system of suddenly changing its configuration under slight changes of the load or the slope at either of the ends.

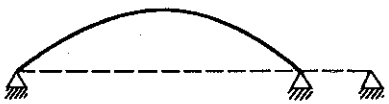

Fig. 1. Beam in postcritical state.

Suitable properties of the flexion springs and their dynamic characteristics in particular, can only be achieved by analysing the dynamics of large

deformations of a beam in a postbuckling state. Complexity of the problem requires a number of simplifying assumptions to be made to derive the solvable motion equations. In the papers devoted to large dynamic deformations, e.g. by WITMER *et al.* [1] and WOODALL [2], rotational mass inertia as well as shear strains were assumed to be negligible. On further assumption that the beam axis undergoes flexure only and its length stays unchanged, the motion equations for arbitrary curvatures take the form

$$\begin{aligned} A\rho\ddot{x} &= (N\cos\varphi - T\sin\varphi)', \\ A\rho\ddot{y} &= (N\sin\varphi + T\cos\varphi)', \end{aligned} \tag{1.1}$$

$$M' = T. \tag{1.2}$$

Load-deformation relationships and auxiliary geometric formualae are

$$M = K\kappa, \tag{1.3}$$

$$\kappa = \varphi', \tag{1.4}$$

$$\operatorname{tg}\varphi = \frac{y'}{x'}, \tag{1.5}$$

where A, ρ, K – cross-sectional area of the beam, its density and flexural stiffness, respectively; x, y – Cartesian coordinates of material points of the beam axis in the $0x0y$ frame of reference; φ – angle between a tangent to the beam axis and the coordinate axis $0x$; κ – beam curvature, N, T, M – components of the internal force tangent and normal to the beam axis and bending moment, respectively. $x, y, \varphi, \kappa, N, T, M$ are functions of a natural coordinate s measured along the beam axis and the time t ($s \in <0, L>$, L – beam length); $(\,)^{\cdot}$ means differentiation with respect to time t, $(\,)'$ means differentiation with respect to the coordinate s.

The presented partial differential equations have no analytical solutions in the literature. WITMER *et al.* [1] modelled the beam as a system of concentrated masses and used the finite difference method. WOODALL [2] introduced an additional simplifying assumption which limited the range of validity of solution to moderately large displacements. The finite difference, the perturbation and the Galerkin methods were used to solve the problem. A similar system for moderately large curvatures and with allowance for rotational inertia was solved with the help of perturbation method by ATLURI [3].

2. Method of solution

Algorithm of numerical solution of the motion equations consists in replacing a continuous structure by a system of rigid elements connected by elastic hinges. Discretization of the beam is shown in Fig.2 whereas the internal forces applied to an element are given in Fig.3 . Each element has a definite length, mass and moment of inertia. The motion of the system

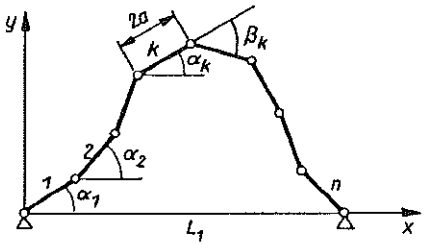

Fig. 2. Discretization of the beam.

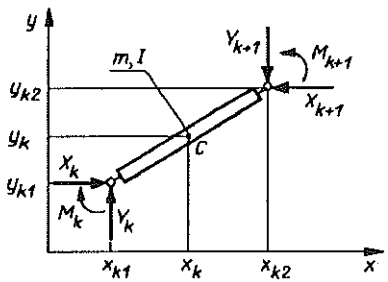

Fig. 3. Rigid element.

is described by the momentum and the moment of momentum conservation principles as well as the internal force-displacement relationships. When the beam axis is inextensible, the relation is limited to the mutual rotation of neighbouring elements and corresponding bending moments. The equations take the form

$$I\ddot{\alpha}_k = M_{k+1} - M_k + (X_k + X_{k+1})a\sin\alpha_k - (Y_k + Y_{k+1})a\cos\alpha_k, \tag{2.1}$$

$$k = 1, 2, \ldots, n,$$

$$\begin{aligned} m\ddot{x}_k &= X_k - X_{k+1}, \qquad k = 1, 2, \ldots, n, \\ m\ddot{y}_k &= Y_k - Y_{k+1}, \qquad k = 1, 2, \ldots, n, \end{aligned} \tag{2.2}$$

$$M_k = K(\alpha_k - \alpha_{k-1}), \qquad k = 2, 3, \ldots, n. \tag{2.3}$$

where $2a$, m, I – length, mass and moment of inertia of an element; X_k, Y_k, M_k – internal forces and moments at the nodes; α_k – angle between the k-th element and the $0x$-axis; x_k, y_k – coordinates of a mass centre for the k-th element; n-number of elements ($L = 2$ an). The initial conditions at $t = t_0$ are

$$\begin{aligned} \alpha_k(t_0) &= \underline{\alpha_k}, \qquad k = 1, 2, \ldots, n, \\ \dot{\alpha}_k(t_0) &= \underline{\dot{\alpha}_k}, \qquad k = 1, 2, \ldots, n, \end{aligned} \tag{2.4}$$

where $\underline{\alpha_k}, \underline{\dot{\alpha}_k}$ – are the initial values of the angles and their rates.

Let the origin of coordinates be at the left-hand side end of the considered beam. The other end lies on the $0x$-axis. Both ends are fixed and cannot move in any direction. The boundary conditions for the beginning of the first element and the end of the last element are

$$x_{1,1} = 0, \qquad y_{1,1} = 0, \tag{2.5}$$

$$x_{n,2} = L_1, \qquad y_{n,2} = 0, \tag{2.6}$$

where $x_{1,1}$, $y_{1,1}$ – coordinates of the left-hand side end of the beam; $x_{n,2}$, $y_{n,2}$ – coordinates of the right-hand side end of the beam; L_1 – distance between the fixed ends of the beam ($L_1 < L$).

Thus the deflections at the beam ends vanish. To have a complete description of the situation, two conditions are still lacking. In what follows two variants of those conditions will be introduced: (1) bending moments conditions and (2) a slope of the left-hand side end the beam associated with the bending moment at the other end.

Since the beam ends are at rest, we have vanishing velocities and accelerations of those points

$$\dot{x}_{1,1} = 0, \qquad \dot{y}_{1,1} = 0, \tag{2.7}$$

$$\ddot{x}_{1,1} = 0, \qquad \ddot{y}_{1,1} = 0, \tag{2.8}$$

$$\dot{x}_{n,2} = 0, \qquad \dot{y}_{n,2} = 0, \tag{2.9}$$

$$\ddot{x}_{n,2} = 0, \qquad \ddot{y}_{n,2} = 0. \tag{2.10}$$

The conditions (2.5), (2.7), (2.8) are satisfied identically since the origin of coordinates coincides with the point concerned. The boundary condition (2.10) referring to the zero acceleration of the end of the beam can be

expressed in terms of the angles α_k

$$
\begin{aligned}
\ddot{x}_{n,2} &= -2a\sum_{k=1}^{n}\left(\dot{\alpha}_k^2\cos\alpha_k+\ddot{\alpha}_k\sin\alpha_k\right)=0\,,\\
\ddot{y}_{n,2} &= -2a\sum_{k=1}^{n}\left(\dot{\alpha}_k^2\sin\alpha_k-\ddot{\alpha}_k\cos\alpha_k\right)=0\,.
\end{aligned}
\tag{2.11}
$$

Similarly, the accelerations $\ddot{x}_k$ and $\ddot{y}_k$ entering Eqs.(2.2), can be shown to take the form

$$
\begin{aligned}
\ddot{x}_k &= -2a\sum_{i=1}^{k-1}\left(\dot{\alpha}_i^2\cos\alpha_i+\ddot{\alpha}_i\sin\alpha_i\right)-a\left(\dot{\alpha}_k^2\cos\alpha_k+\ddot{\alpha}_k\sin\alpha_k\right),\\
\ddot{y}_k &= -2a\sum_{i=1}^{k-1}\left(\dot{\alpha}_i^2\sin\alpha_i-\ddot{\alpha}_i\cos\alpha_i\right)-a\left(\dot{\alpha}_k^2\sin\alpha_k-\ddot{\alpha}_k\cos\alpha_k\right).
\end{aligned}
\tag{2.12}
$$

The system of equations consists of the motion equations (2.1), (2.2), elasticity relationships (2.3) and the acceleration boundary condition at the end of the beam (2.10). Linear accelerations $\ddot{x}_k$, $\ddot{y}_k$ in Eqs.(2.2) and (2.10) may be eliminated since they are expressed in terms of angles α_k and their derivatives $\dot{\alpha}_k$ and $\ddot{\alpha}_k$, (2.12) and (2.11). We finally get:

$$
\begin{aligned}
&I\ddot{\alpha}_k = M_{k+1}-M_k+(X_k+X_{k+1})a\sin\alpha_k\\
&\qquad -(Y_k+Y_{k+1})a\cos\alpha_k, \qquad k=1,2,\ldots,n,\\
&m\left[-2a\sum_{i=1}^{k-1}\left(\dot{\alpha}_i^2\cos\alpha_i+\ddot{\alpha}_i\sin\alpha_i\right)-a\left(\dot{\alpha}_k^2\cos\alpha_k+\ddot{\alpha}_k\sin\alpha_k\right)\right]\\
&\qquad = X_k-X_{k+1}, \qquad k=1,2,\ldots,n,\\
&m\left[-2a\sum_{i=1}^{k-1}\left(\dot{\alpha}_i^2\sin\alpha_i-\ddot{\alpha}_i\cos\alpha_i\right)-a\left(\dot{\alpha}_k^2\sin\alpha_k-\ddot{\alpha}_k\cos\alpha_k\right)\right]\\
&\qquad = Y_k-Y_{k+1}, \qquad k=1,2,\ldots,n,\\
&M_k = K(\alpha_k-\alpha_{k-1}), \qquad k=2,3,\ldots,n,\\
&-2a\sum_{k=1}^{n}\left(\dot{\alpha}_k^2\cos\alpha_k+\ddot{\alpha}_k\sin\alpha_k\right)=0,\\
&-2a\sum_{k=1}^{n}\left(\dot{\alpha}_k^2\sin\alpha_k-\ddot{\alpha}_k\cos\alpha_k\right)=0.
\end{aligned}
\tag{2.13}
$$

The above system constitutes $4n+1$ algebraic equations that are linear with respect to $\ddot{\alpha}_k$, X_k, Y_k, M_k, X_{n+1}, Y_{n+1}, M_{n+1} $(k = 1, 2, \ldots, n)$. The number of these quantities is $4n+3$. If two of the above listed quantities are known, the number of equations becomes equal to the number of unknowns and a unique solution can be arrived at, provided the principal matrix of the system is not singular. This means that, knowing at a given time instant t the configuration of elements, their velocities and two values from the above $4n+3$ accelerations, forces and moments, remaining quantities can be found in a nonsingular situation. The two mentioned quantities supplement the description of boundary conditions. In the system of Eqs.(2.13) the values M_1, M_{n+1} can be chosen as known ones. This corresponds to a statical input of known applied moments at the ends of the beam. The kinematic input can be modelled by assuming $\ddot{\alpha}_1(t)$. This means a description of the motion of the beam under forcing function $\alpha_1(t)$ resulting from the known function $\ddot{\alpha}_1(t)$ and an initial value of $\dot{\alpha}_1(t_0)$.

The system (2.13) can be solved for the accelerations $\ddot{\alpha}_k$. By numerical integration approximate values of velocities $\dot{\alpha}_k$ and the angles α_k themselves are obtained in the next time step. However, the angles α_k and angular velocities $\dot{\alpha}_k$ will not, in general, satisfy the boundary conditions (2.6) and (2.9) for a location and velocity of the end of the beam. By assuming adequately small time step the values of α_k and $\dot{\alpha}_k$ differ little from those that satisfy the boundary conditions in an exact manner. That is why the obtained values of α_k and $\dot{\alpha}_k$ are corrected in order to satisfy the conditions (2.6) and (2.9) with the least error possible. At the same time, the corrections must be small enough not to distort the whole solution.

One of the procedures to approach the above described problem is, in the first place, to try to obtain a location of the beam end according to the condition (2.6). On the basis of the angles α_k we calculate the kinking angles β_k $(k = 1, 2, \ldots, n-1)$ between the neighbouring rigid elements, Fig.2.

$$\beta_k = \alpha_{k+1} - \alpha_k, \qquad k = 1, 2, \ldots, n-1. \tag{2.14}$$

By uniform increase of absolute values of the kinking angles at all hinges, the distance between the ends of the chain of rigid elements becomes smaller. Conversely, by a decrease of absolute values of the kinking angles the chain becomes more straight and its end depart. After the desired distance between the ends is reached, the whole chain is subject to a rigid rotation with respect to the origin of the coordinate system until its right-hand side end touches the $0x$-axis. This procedure enables the condition (2.6) to be

satisfied to within a required accuracy, limited by the precision of arithmetic operations. When the angles α_k satisfying (2.6) are known, the second stage of the correction follows by seeking such corrections η_k for the velocities $\dot{\alpha}_k$ that will result in the satisfaction of the condition (2.9) on the vanishing velocity at the support. The following equations must be met:

$$
\begin{aligned}
2a\sum_{k=1}^{n}(\dot{\alpha}_k+\eta_k)\sin\alpha_k &= 0, \qquad k=1,2,\ldots,n,\\
2a\sum_{k=1}^{n}(\dot{\alpha}_k+\eta_k)\cos\alpha_k &= 0, \qquad k=1,2,\ldots,n,
\end{aligned}
\tag{2.15}
$$

where η_k denote corrections for the angular velocities $\dot{\alpha}_k$. The correction η_k can be minimized by using various norms. Minimum of squared corrections is required in further calculations,

$$
\sum_{k=1}^{n}\eta_k^2=\min. \tag{2.16}
$$

On using the Lagrange method, the minimum of correction function is sought

$$
H=\sum_{k=1}^{n}\eta_k^2+\lambda_1\sum_{k=1}^{n}(\dot{\alpha}_k+\eta_k)\sin\alpha_k+\lambda_2\sum_{k=1}^{n}(\dot{\alpha}_k+\eta_k)\cos\alpha_k, \tag{2.17}
$$

where λ_1, λ_2 are the Lagrange multipliers.

The condition

$$
\frac{\partial H}{\partial\eta_k}=0, \qquad k=1,2,\ldots,n \tag{2.18}
$$

provides expressions for η_k that, after substituting into (2.15), enable the multipliers λ_1, λ_2 to be calculated followed by the corrections η_k themselves. Knowing the configuration and the velocities, subsequent calculations are conducted by repeating the described algorithm for the consecutive time instants.

A considerable decrease in the principal matrix order, and thus reducing the dimensions of the computational task, can be readily achieved by using Eqs.(2.2) and (2.3) in Eq.(2.1). In this way n forces X_k, n forces Y_k and $n-1$ moments M_k $(k=1,2,\ldots,n+1)$ can be eliminated from Eq.(2.1). There remain $n+2$ equations containing n accelerations $\ddot{\alpha}_k$ $(k=1,2,\ldots,n)$, two single values of X_i, Y_i and two values of M_i $(1\leq i\leq n+1)$. Accepting as known two from among these magnitudes, we again arrive at the same number of equations and unknowns, i.e. $(n+2)$.

3. Statics of the beam

If damping terms are accounted for in the motion equations (e.g. expressed as linear functions of velocities) the presented algorithm can be employed in statical analysis of the beam with the use of the dynamic relaxation method [4, 5]. Due to the action of viscous damping the system tends asymptotically to its statical equilibrium configuration, which usually happens after a suitable time of vibration damping has elapsed.

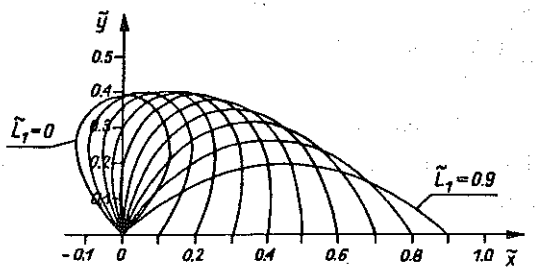

Fig. 4. Beam in static equilibrium.

Deformed beam axes under static equilibrium for various parameters $\tilde{L}_1 = L_1/L$ ranging from 0 to 0.9 are depicted in Fig.4. The solutions were obtained on assuming that $M_1 = 0$ and $M_{n+1} = 0$. Equilibrium configurations are shown in the dimensionless coordinates $\tilde{x} = x/L$ and $\tilde{y} = y/L$. The analysed beam was split up into $n = 20$ elements. Broken lines for particular configurations of rigid elements represent the elastic axes in a satisfactory manner as compared with exact analytical solutions.

Load-displacement characteristics of three flat springs for the end distance parameters $\tilde{L}_1 = 0.4$, 0.6 and 0.8 are shown in Fig.5. The springs were modelled as beams in the postcritical states having the initial configurations such as shown in Fig.4. A dimensionless slope parameter $\tilde{\alpha}_1$ denotes a change in the slope of the left-hand side end of the beam with respect to its initial value,

$$\tilde{\alpha}_1 = \frac{\alpha_{1,0} - \alpha_1}{\alpha_{1,0}}, \tag{3.1}$$

where $\alpha_{1,0}$ – slope of a beam before load is applied, α_1 – slope of the loaded beam. The other, vertical coordinate of the diagram denotes a dimensionless applied moment

$$\tilde{M}_1 = \frac{M_1 L}{EI}. \tag{3.2}$$

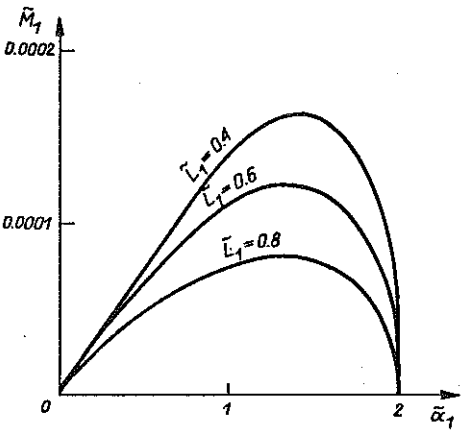

FIG. 5. Static characteristics.

The presented characteristics are obtained under kinematic excitation. For a fixed value of the angle α_1, and after a sufficient damping of vibrations has taken place, the applied moments were found via the equilibrium equations of the system. The calculations were made for the angle α_1 varying from its value resulting from the equilibrium state with no load $\alpha_{1,0}$ to the value $-\alpha_{1,0}$ for a configuration symmetric with respect to the initial configuration. The dimensionless slope parameter $\tilde{\alpha}_1$ takes the values between 0 and 2. Figure 5 shows a strong nonlinearity of the characteristics. At the final stage of the deformation process (i.e. for α_1), approaching $-\alpha_{1,0}$, the moment M_1 rapidly decreases and an abrupt change of configuration occurs. In this state the beam becomes in equilibrium again when $M_1 = 0$.

4. DYNAMICS OF THE BEAM

A series of deformation patterns of the beam in the postcritical state is shown in Fig.6 a-h. The torque

$$M_1(t) = M_{1,0}\eta(t) \tag{4.1}$$

was applied to one of the beam ends. $M_{1,0}$ denotes the load amplitude, $\eta(t)$ stands for Heaviside's step function. The nondimensional load amplitude is $M_1 = 1.19 \times 10^{-4}$. Initially the unloaded beam was in the static equilibrium and the parameter of the ends distance was $\tilde{L}_1 = 0.8$. Consecutive configurations of the beam were registered every 3 ms. Numerical integration

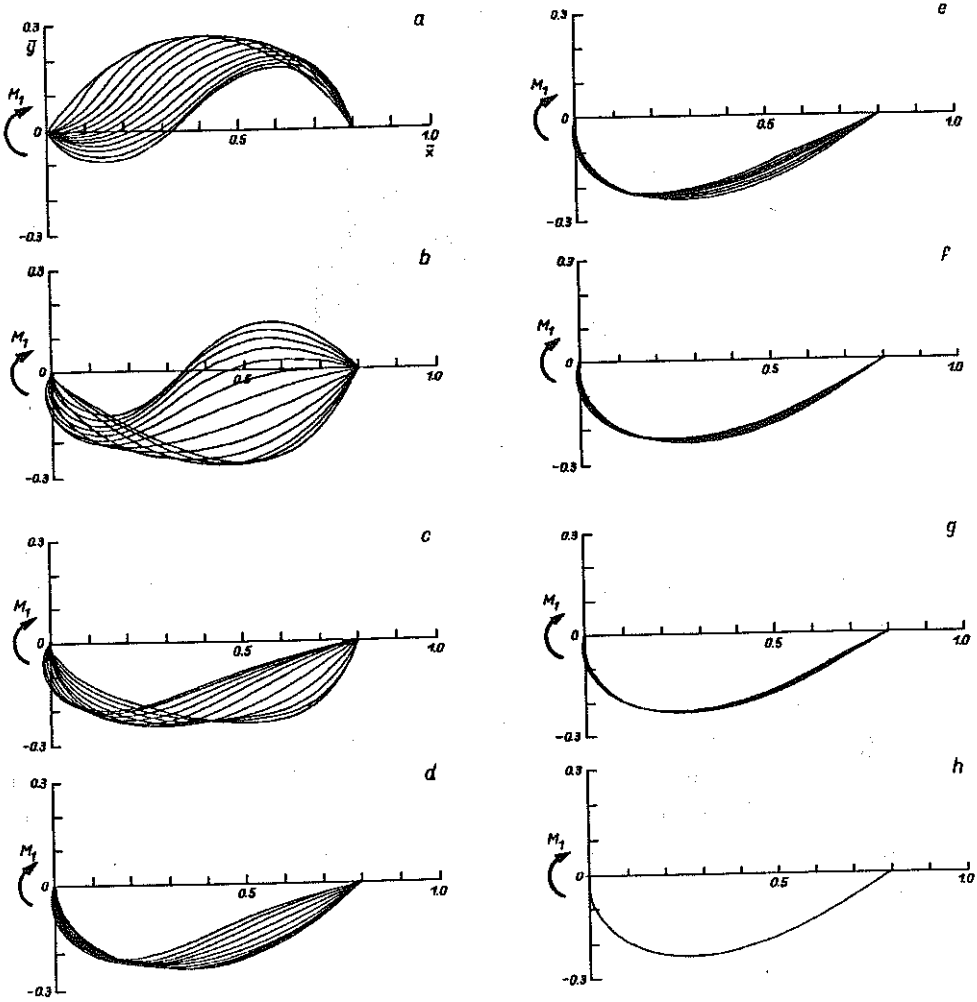

FIG. 6. Beam deflections in a postcritical state.

was made by the Runge-Kutta method of the fourth order. The applied damping enabled the change of configuration to be studied from the start to the final static equilibrium configuration.

Time-dependent slopes α_1 and α_n of the first and the last element of the beam are shown in Fig.7. The deformation process was similar to that visualized in Fig.6, i.e. an abrupt loading of a beam in its postcritical state ($\tilde{L}_1 = 0.8$) by a moment $\tilde{M}_1 = 8.93 \times 10^{-5}$ in the presence of damping. Figures 6 and 7 show the complexity of the deformation history. In Fig.7

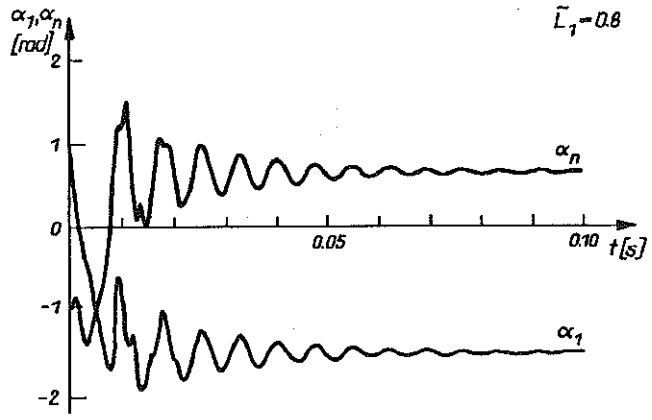

FIG. 7. Response of a system to an abrupt static input.

slight disturbances can be seen imposed on the fundamental mode of motion. They correspond to the propagation of bending waves along the beam.

Responses of the system to the kinematic excitation are shown in Figs.8--10. A beam in the postcritical state was deformed according to the given function of the slope $\alpha_1(t)$. The input was distributed during the first 0.03 s in a linear manner between the slopes associated with symmetric configurations of the statical equilibrium. Later the load functions remains constant. Response of the considered system is illustrated with the help of the time-dependent distribution of the end slope $\alpha_n(t)$. The presented diagrams refer to the end distance parameters $\tilde{L}_1 = 0.8$, 0.6 and 0.4. Starting from an instant when the slope of the beginning of the beam becomes opposite to the

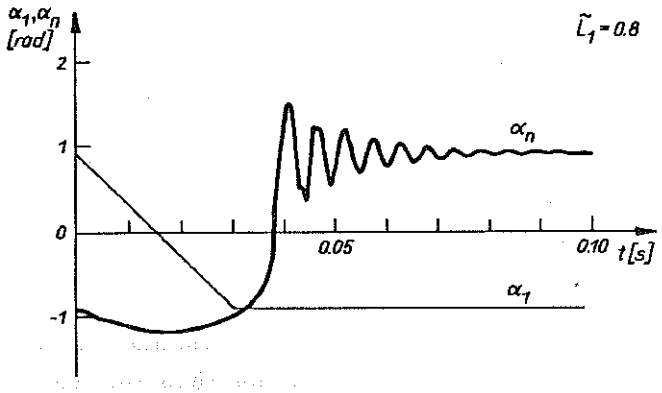

FIG. 8. Response of a system to a kinematic input for $\tilde{L}_1 = 0.8$.

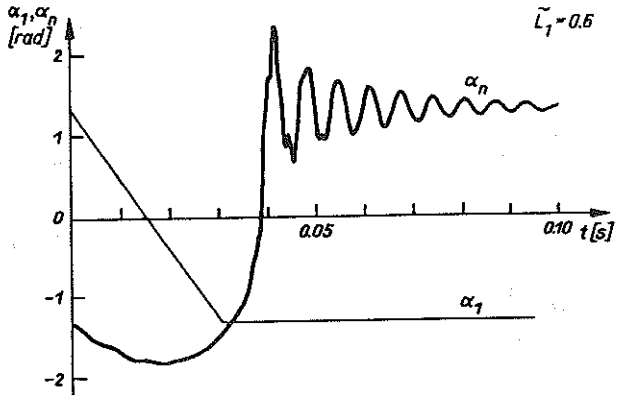

FIG. 9. Response of a system to a kinematic input for $\tilde{L}_1 = 0.6$.

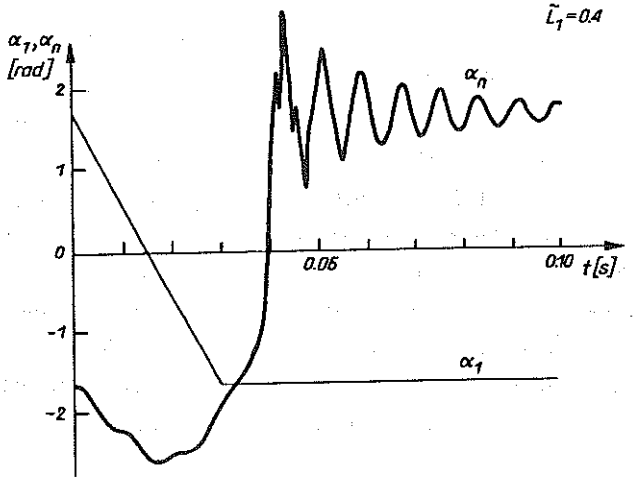

FIG. 10. Response of a system to a kinematic input for $\tilde{L}_1 = 0.4$.

initial one, the change of configuration of the system becomes exceedingly abrupt. Again, propagation of flexural wave can be observed.

5. SUMMING UP

A method is presented for analysing large dynamic deformations of beams whose end hinges are closer to each other than the length of the beam itself. The method consists in the discretization of the system, inclusion of the constraint equations to the motion equations, numerical integration

of accelerations at each time step and the analytical-numerical corrections of the approximate solutions in order to satisfy the boundary conditions optimally. The proposed procedure enables to analyse complex dynamic problems at a relatively low cost. Moreover, broad possibilities seem to exist to develop the method and apply it to other physically nonlinear systems. One of the present authors is preparing a paper devoted to the numerical properties of the algorithm and experimental verification of the obtained results.

REFERENCES

1. E.A.WITMER, H.A.BALMER, J.W.LEECH, T.H.H.PIAN, *Large dynamic deformations of beams, rings, plates, and shells*, AIAA J., 1, 1848, 1963.
2. S.R.WOODALL, *On the large amplitude oscillations of a thin elastic beam*, Int. J. Non-linear Mechanics, 1, 217, 1966.
3. S.ATLURI, *Nonlinear vibrations of a hinged beam including nonlinear inertia effects*, J. of Applied Mech., 40,121, 1973.
4. J.R.H.OTTER, *Computations for prestressed concrete reactor pressure vessels using dynamic relaxation*, Nuclear Structural Engng., 1, 61, 1965.
5. J.W.BUNCE, E.H.BROWN, *Non-linear bending of thin, ideally elastic rods*, Int. J. Mech. Sci., 18, 435, 1976.

POLISH ACADEMY OF SCIENCES
INSTITUTE OF FUNDAMENTAL TECHNOLOGICAL RESEARCH, WARSZAWA.

Received March 11, 1992.